Journal-Ref: Astronomy Letters, 2006, v. 32, No 10, pp. 649-660

Estimating the Dark Halo Mass from the Relative Thickness of Stellar Disks

N.Ya. Sotnikova (nsot@astro.spbu.ru)
S.A. Rodionov (seger@astro.spbu.ru)

Sobolev Astronomical Institute, St. Petersburg State University, St. Petersburg

We analyze the relationship between the mass of a spherical component and the minimum possible thickness of stable stellar disks. This relationship for real galaxies allows the lower limit on the dark halo mass to be estimated (the thinner the stable stellar disk is, the more massive the dark halo must be). In our analysis, we use both theoretical relations and numerical N-body simulations of the dynamical evolution of thin disks in the presence of spherical components with different density profiles and different masses. We conclude that the theoretical relationship between the thickness of disk galaxies and the mass of their spherical components is a lower envelope for the model data points. We recommend using this theoretical relationship to estimate the lower limit for the dark halo mass in galaxies. The estimate obtained turns out to be weak. Even for the thinnest galaxies, the dark halo mass within four exponential disk scale lengths must be more than one stellar disk mass.

1 Introduction

A large body of observational data provides evidence for the existence of dark matter, which manifests itself only through its gravitational influence on stellar systems of various scales (from individual galaxies to clusters of galaxies and superclusters), determining to a great extent their dynamics and structure. The controversy surrounding the following two main questions related to the dark matter is still continuing: What is its nature and to what extent does it exceed in mass the luminous matter? The first question is far from being resolved. As regards the second question, on the scales of individual galaxies, it is formulated as follows: Beginning from which regions (inner or outer) does the dark halo mass prevail over the luminous mass?

There are several observational constraints on the mass and extent of the dark halos in galaxies; these constraints do not depend on what the nature of the dark matter is. In general, they give an estimate of the lower limit for the dark halo mass within a fixed radius. For spiral galaxies, this estimate primarily follows from the analysis of the contributions from various components of the system to its rotation curve for the so-called maximum disk model (a classical example of the separation of the contributions from the disk and the dark halo to the rotation curve of a galaxy, NGC 3198; van Albada et al. 1985). In this model, the dark halo mass within the optical radius of a galaxy generally does not exceed the stellar disk mass. When specific systems are investigated, a joint interpretation of the data on the rotation curves and radial velocity dispersion profiles, along with considerations regarding the marginal stability of stellar disks (see, e.g., Bottema and Gerritsen 1997; Khoperskov et al. 2001; Zasov et al. 2001; Khoperskov and Tyurina 2003)[1], often raises significantly the lower limit for the dark halo mass within a fixed radius (occasionally, interpretation of the data on the stellar velocity dispersion based on numerical simulations increases the dark halo mass by almost an order of magnitude compared to its value given by the maximum disk model[2]).

The upper limit for the dark halo mass is much more difficult to constrain. Where the region within the optical radius of a galaxy is involved, stability-related considerations are invoked. For example, the presence of a regular spiral pattern related to the propagation of density waves in galaxies requires a gravitationally "active" stellar disk, which reduces the contribution from the spherical component to the total gravitational field of the spiral galaxy and to the total mass (Athanassoula et al. 1987). Another important test for the presence of a massive halo is the length of the tidal tails in interacting spiral galaxies. In interacting systems, we quite often observe extended tidal features stretching to distances as large as 40–100 kpc. Based on numerical simulations of interacting disk galaxies with dark halos that correspond to models obtained in cosmological calculations (Navarro et al. 1999), Dubinski et al. (1999) showed that the calculated parameters could be reconciled with the parameters of observed systems only for two types of models: models with an extended moderate-mass halo and a rotation curve that is determined almost entirely by the stellar disk within the optical radius and models with a compact low-mass halo that makes the main contribution to the rotation curve in the inner disk. Reconciling

[1] In these papers, the results of numerical N-body simulations with a variable disk mass were used to explain the observed stellar velocity dispersion for a number of spiral galaxies.

[2] The galaxy NGC 891 may be cited as an example (Khoperskov et al. 2001).

the rotation curves of specific interacting systems (e.g., NGC 4038/39 and NGC 7252) and the sizes of their tidal features with the model parameters leads one to conclude that the stellar disks in such systems dominate in mass within the optical radius, which gives a strong upper limit on the dark mass. A similar conclusion was also drawn from the simulations of the famous Mice galaxy, NGC 4676 (Sotnikova and Reshetnikov 1998).

Comparison of the various estimates for the dark mass in galaxies shows that the upper and lower limits do not overlap (see, e.g., McGaugh and Block 1998). This gives reason to revise a number of tests, in particular, the test related to the thickness of the stellar disks in spiral galaxies suggested by Zasov et al. (1991, 2002). These authors argue that the thickness of a stable stellar disk at a given halo mass is limited below. If the disk thickness is smaller than a certain value, then bending instability will lead to increasing the vertical velocity dispersion and to a thickening of the system. The growth of bending perturbations is stabilized by a massive dark halo: the more massive the halo is, the thinner the stable disk can be. As we showed previously (Sotnikova and Rodionov 2005), not only a massive dark halo has a stabilizing effect on the growth of bending perturbations, leaving the stellar disk fairly thin. A low-mass compact bulge also produces such an effect. In this case, the lower limits on the dark mass can be mild and consistent with the upper limits. In this paper, we analyze the relationship between the stellar disk thickness and the dark halo mass that is derived both from theoretical considerations and from numerical simulations of the dynamical evolution of thin disks in the presence of spherical components with different density profiles and different masses. The derived relationship predicts moderate dark halo masses even for the thinnest galaxies.

2 The stellar disk thickness and the relative mass of the spherical component

When the global parameters of stellar disks are analyzed, the disks are generally assumed to be stable against the growth of perturbations in the plane and in the vertical direction. The stability conditions for a given dark halo mass limit below the radial and vertical stellar velocity dispersions. Since the vertical velocity dispersion is related to the stellar disk thickness, it is also limited below at a fixed dark halo mass.

The disks are commonly assumed to be at the stability boundary. In this case, the relative stellar disk thickness and the relative dark halo mass are related to one another. This relationship was (probably first) noticed by Zasov et al. (1991) on the following grounds.

For a gravitating layer with a volume density profile that corresponds to an isothermal (along the z axis) model (Spitzer 1942),

$$\rho(z) = \frac{\Sigma}{2z_0}\,\mathrm{sech}^2(z/z_0)\,, \tag{1}$$

the following relation, which is a vertical equilibrium condition, is known to be valid:

$$\sigma_z^2 = \pi G z_0 \Sigma\,. \tag{2}$$

Here, Σ is the star surface density of the layer, z_0 is the scale length of the density variations in the z direction, and σ_z^2 is the vertical stellar velocity dispersion of the layer. If condition (2) is applied to a stellar disk, then the R dependences of Σ, z_0, and σ_z should be taken into account. For real stellar disks embedded in a dark halo, the vertical equilibrium condition must be defined slightly differently (Bahcall 1984). However, as was shown, for example, by Rodionov and Sotnikova (2006), the approximation of isothermal layers holds good for the entire disk except the innermost regions even in the presence of a massive spherical component.

If the disk is stable against perturbations in the plane, then the root-mean-square (rms) radial velocity must be

$$\sigma_R(R) = Q_{\rm T}\,\frac{3.36\,G\,\Sigma(R)}{\kappa(R)}\,, \tag{3}$$

where $Q_{\rm T}\gtrsim 1$ is the Toomre parameter, $\kappa = \sqrt{2\left(\frac{v_{\rm c}^2}{R^2} + \frac{v_{\rm c}}{R}\frac{dv_{\rm c}}{dR}\right)}$ is the epicyclic frequency, and $v_{\rm c}$ is the linear circular velocity. The coefficient 3.36 in Eq.(3) corresponds to an infinitely thin model disk (Toomre 1964).

An expression for the minimum possible relative thickness of a stable disk can be derived from equilibrium condition (2) and stability condition (3). To be able to compare theoretical estimates with observational data, let us write the expression for the relative disk thickness at a certain radius, for example, $R = 2h$, where h is the exponential radial disk scale length, which enters into the commonly used law of surface density variations with radius:

$$\Sigma(R) = \frac{M_{\rm d}}{2\pi h^2}\exp\left(-R/h\right),$$

where $M_{\rm d}$ is the total disk mass. The radius $2h$ was chosen on the grounds that the observed vertical disk structure in this region is generally no longer distorted by the central bulge, the bar, and the so-called X-shaped structures.

At $R\gtrsim 2h$, the rotation curves of luminous galaxies generally reach a plateau. In this case, the epicyclic frequency (see stability condition (3)) is related to the linear circular velocity $v_{\rm c}$ by $\kappa(R) = \sqrt{2}v_{\rm c}/R$. In the plateau region, $v_{\rm c}$ is roughly constant and, hence, $v_{\rm c}(2h) \approx v_{\rm c}(4h)$. We can then use $v_{\rm c}$ to estimate the total mass of a galaxy (including the mass of its spherical component $M_{\rm sph}$) within a fixed radius, for example, $R = 4h$, $M_{\rm tot}(4h) \approx 4hv_{\rm c}^2/G$ (see, e.g., Zasov et al. 2002). In addition, the marginal stability condition in the disk plane allows $Q_{\rm T}$ to be chosen almost uniquely. Based on numerical N-body simulations, Khoperskov et al. (2003) showed that $Q_{\rm T}$ at $R \simeq (1-2)h$ for marginally stable 3D stellar disks is equal to a nearly constant value of $1.2-1.5$, which does not depend on the relative mass of the spherical component. Based on the results of Khoperskov et al. (2003), we took $Q_{\rm T}(2h) \approx 1.4$. Using Eqs.(2) and (3), under our additional assumptions, we then obtain

$$\frac{z_0(2h)}{h} \approx 1.2\,\frac{\sigma_z^2}{\sigma_R^2}\,\frac{M_{\rm d}}{M_{\rm tot}(4h)}\,. \tag{4}$$

If we fix the ratio σ_z/σ_R at the level given by the local linear criterion for bending instability, i.e., at approximately $0.29-0.37$ (Toomre 1966; Kulsrud et al. 1971; Poly-

achenko and Shukhman 1977; Araki 1985), then, according to Eq.(4), the relative stellar disk thickness measured at the given distance $R = 2h$ is

$$\frac{z_0(2h)}{h} \approx \frac{0.18}{1+\mu(4h)}\,, \tag{5}$$

where $\mu(4h) = M_{\rm sph}(4h)/M_{\rm d}(4h)$, $M_{\rm tot}(4h) = M_{\rm d}(4h) + M_{\rm sph}(4h)$, $M_{\rm sph}(4h)$ – mass of spheroidal component. In (5), we took into account the fact that 90% of the disk mass is contained within $4h$ for an exponential surface density profile. The numerical coefficient in Eq.(5) was obtained for $\sigma_z/\sigma_R = 0.37$ (this value corresponds to the linear criterion for bending instability in Polyachenko and Shukhman (1977)). The larger the relative mass of the spherical component within a fixed radius, for example, $4h$, the smaller the relative disk thickness $z_0(2h)/h$ at this radius. The latter conclusion is one of the main conclusions reached by Zasov et al. (1991). In the conclusion under discussion the coefficient in relation (5) will be of interest in the subsequent analysis.

Equation (5) was derived for the specific law of density variations in the vertical direction (1). In certain cases, the vertical volume density profile of the disk matter is fitted by other laws (van der Kruit 1988), for example,

$$\rho(z) = \frac{\Sigma}{\pi z_e}\,{\rm sech}(z/z_e) \tag{6}$$

or an exponential law,

$$\rho(z) = \frac{\Sigma}{2h_z}\,\exp(-|z|/h_z)\,, \tag{7}$$

where z_e and h_z are the corresponding vertical scale heights that can depend on R. It can be shown that an equilibrium condition similar (2) for profiles (6) or (7) may be written as

$$< \sigma_z^2 >= C\pi G\Delta\Sigma\,, \tag{8}$$

where $< \sigma_z^2 >$ where is the vertical velocity dispersion averaged along the z axis; Δ is the half-thickness of a homogeneous layer with a density equal to the density in the disk at $z = 0$; and $C = 1$, $C = 28\,\zeta(3)/\pi^3 \approx 1.0854$ (ζ is the Riemann function), and $C = 1.5$, respectively[3], for density profiles (1), (6), and (7). Below, we argue that the vertical profiles of model disks at late evolutionary stages are more likely described by laws (2) or (6) than by (7). In this case, $C \approx 1.0-1.1$ in equilibrium condition (8) and the numerical coefficient in (5) is virtually constant if Δ, the half-thickness of a homogeneous layer[4], is used in place of z_0.

Note that relation (5) is valid for a marginally stable stellar disk. If a galaxy has a margin of stability against perturbations in the plane or against bending perturbations, then the greater sign must be substituted for the sign of approximate equality in (5). As

[3]To obtain these coefficients, we must substitute the corresponding laws of density variations in the Jeans equation that describes the vertical equilibrium and, having calculated the law of velocity dispersion variations along z, average this quantity.

[4]For density profile (8), the vertical scale height z_0 is exactly equal to the half-thickness of a homogeneous layer Δ.

a result, for stable stellar disks, Eq.(5) yields

$$\mu(4h) \gtrsim 0.18 \frac{h}{z_0(2h)} - 1\,. \tag{9}$$

The lower limit for the mass of the spherical component in a galaxy, in particular, the dark halo mass, can be estimated from the observed relative thickness of the galaxy using relation (9). Note that the theoretical estimate is weak. Even for extremely thin galaxies with $z_0/h = 1/15$, we find that $\mu(4h)\gtrsim 1.7$. For example, for the thinnest galaxy in the sample that was used by Zasov et al. (2002), $z_0/h \approx 1/11$ (see Fig.4b in this paper). For such a galaxy, according to (9), $\mu(4h)\gtrsim 0.98$. In the sample of edge-on galaxies whose parameters were discussed by Kregel et al. (2002), $z_0/h \approx 1/9.7$ for the thinnest galaxy (435-G25) (see Table 1 in this paper)[5]. For such a galaxy, Eq.(9) yields $\mu(4h)\gtrsim 0.75$.

3 Numerical simulations

The relationship between the relative stellar disk thickness and the relative dark halo mass derived from five N-body simulations was also first discussed by Zasov et al. (1991). A similar relationship was constructed by Mikhailova et al. (2001) using several tens of simulations. In general, the two relationships coincide.

It should be noted that theoretical relation (5) written above was derived from the considerations that were used to substantiate the results of N-body simulations (Zasov et al. 1991, 2002). However, even a superficial comparative analysis shows that the curve corresponding to theoretical relation (5) lies well below the curve constructed from the experimental data points (see Fig.2 in Mikhailova et al. (2001)). According to the analytical studies of various authors, the factor σ_z/σ_R appearing in Eq.(4) lies within the range $0.29 - 0.37$. We took the maximum value of this factor, 0.37. If we took a smaller velocity dispersion ratio, then the differences between the theoretical curve and the experimental data points would be even larger.

The relationship analyzed by Zasov et al. (1991) and Mikhailova et al. (2001) can be roughly approximated by the formula $(0.3-0.35)/(1+\mu(4h))$. Thus, the thickness of the numerical stellar disk models is approximately twice the thickness calculated using (5). In other words, the relationship derived from N-body simulations predicts a higher dark halo mass than estimate (9). In our view, this discrepancy makes it difficult to interpret both the results of numerical simulations and the relationships derived from observational data (Zasov et al. 2002) and requires a more refined analysis of the numerical simulations that primarily includes the stabilizing role of a compact low-mass spherical component (Sotnikova and Rodionov 2005).

3.1 Numerical Models

Below, we analyze the parameters of several tens of models that we obtained from numerical N-body simulations. We used an algorithm based on the hierarchical tree algo-

[5]In this paper, exponential profile (7) was used to fit the vertical stellar disk density profile. The vertical scale height was defined by h_z, which, according to the authors themselves, is related to z_0 for density profile (1) by $h_z = 0.5 z_0$.

rithm (Barnes and Hut 1986) and some of the codes from the NEMO software package (http:astro.udm.edu/nemo; Teuben 1995).

The stellar disk was represented by a system of N gravitating bodies (N was varied within the range 300 000 to 500 000) and the spherically symmetric component was described in terms of an external static potential that was a superposition of two potentials, the bulge and the dark halo.

The initial particle velocities (the rotational and random velocities) were specified on the basis of equilibrium Jeans equations using a standard technique (see, e.g., Hernquist 1993). A description of the method for constructing the initial model can be found in our previous papers (Sotnikova and Rodionov 2003, 2005). Also given there are the details concerning the bulge model (a Plummer sphere) and the halo model (a logarithmic potential).

The ratio of the mass of the spherical component to the disk mass within $4h$ was varied between 0.25 and 4. The mass of the spherical component was distributed differently between the bulge and the halo. The scale length of the bulge was chosen to be $a_\mathrm{b} = h/7$ almost for all models. We also considered models with concentrated ($a_\mathrm{h} = h/1.75$) and "loose" ($a_\mathrm{h} = h/0.35$) halos, a_h is the scale length of the mass distribution in the halo. The potential softening length ϵ for all models corresponded to our recommendations given previously (Rodionov and Sotnikova 2005), $\epsilon = h/175$.

For all models, we chose nearly equilibrium (in the radial and vertical directions), but unstable (against the growth of bending perturbations) initial conditions. During the growth of bending instability, the system was dynamically heated, the velocity dispersion increased in the z direction, and the disk thickness increased to a value close to the lower boundary of a steady state. The main parameter in which the stellar disk models being analyzed differ is the fraction of the total mass of the galaxy contained in its spherical component (the dark halo and the bulge).

3.2 Determining the stellar disk thickness in numerical simulations

Before discussing in detail the relationship between the relative stellar disk thickness and the relative dark halo mass in galaxies, we should gain an understanding of how the thickness of numerically simulated disks is determined. For model disks, the thickness at a given distance R from the disk center is usually estimated as the rms deviation of the z coordinates of stars from the symmetry plane of the disk (see, e.g., Khoperskov and Tyurina 2003):

$$z_\mathrm{rms} = \sqrt{\left\langle (z - < z >)^2 \right\rangle}\,. \tag{10}$$

The disk in the z direction is commonly assumed to have volume density profile (1) that corresponds to an isothermal model. In this case, z_0 and z_rms are related by

$$z_0 = \frac{2\sqrt{3}}{\pi}\, z_\mathrm{rms} \approx 1.10\, z_\mathrm{rms}\,. \tag{11}$$

For density profile (1), z_0 is the half-thickness of a homogeneous layer, Δ, with the volume density at $z = 0$. The parameter z_0 is estimated from observational data for real

galaxies by analyzing how the surface brightness of the edge-on stellar disk varies along the z axis and by fitting the brightness distribution to $\propto \mathrm{sech}^2(z/z_0)$. Based on (11), one can assume that the parameter $z_{\rm rms}$ determined from (10) for numerical models quantitatively differs only slightly from the disk half-thickness z_0 appearing in law (1) and characterizes the thickness of real disk galaxies. However, we will now show that in practice $z_{\rm rms}$ is a poor characteristic of the model disk thickness and that using it can lead to incorrect relations between the stellar disk thickness and other global parameters of spiral galaxies.

A certain number of particles that fly far away from the disk plane appear in a model galaxy during its evolution. Since their number is small, the z particle distribution is generally well fitted by isothermal density profile (1). However, this small number of distant particles contributes significantly to $z_{\rm rms}$ and leads to an overestimation of the stellar disk thickness calculated in this way. The extent to which the thickness is overestimated depends on the relative mass of the spherical component and on the distance from the center at which we measure the thickness.

Let us introduce another parameter that can characterize the thickness of model stellar disks at a given distance R: $z_{1/2}$ — the median of the absolute value of z. Twice $z_{1/2}$ is the thickness of the layer within which one half of the particles is contained. For density profile (1), based on the introduced definitions, we have

$$\begin{aligned} \Delta &= z_0\,, \\ \frac{\Delta}{2z_{1/2}} &= \frac{1}{\ln 3} \approx 0.91\,, \\ \frac{z_{\rm rms}}{2z_{1/2}} &= \frac{\pi}{2\sqrt{3}\ln 3} \approx 0.83\,. \end{aligned} \tag{12}$$

It is easy to show that the relations between $z_{1/2}$, Δ, and $z_{\rm rms}$ for density profile (6) and (7) can be written as follows: for (6),

$$\begin{aligned} \Delta &= z_{\rm rms} = \frac{\pi}{2}\, z_e\,, \\ \frac{\Delta}{2z_{1/2}} &= \frac{\pi}{4\ln\left(\tan\dfrac{3\pi}{8}\right)} \approx 0.89\,, \\ \frac{z_{\rm rms}}{2z_{1/2}} &\approx 0.89\,, \end{aligned} \tag{13}$$

and for (7),

$$\begin{aligned} \Delta &= \frac{\sqrt{2}}{2}\, z_{\rm rms} = h_z\,, \\ \frac{\Delta}{2z_{1/2}} &= \frac{1}{2\ln 2} \approx 0.72\,, \\ \frac{z_{\rm rms}}{2z_{1/2}} &= \frac{1}{\sqrt{2}\ln 2} \approx 1.02\,. \end{aligned} \tag{14}$$

These relations allow us to check how adequately the introduced parameters describe the model disk thickness and to reach certain conclusions regarding the law by which the

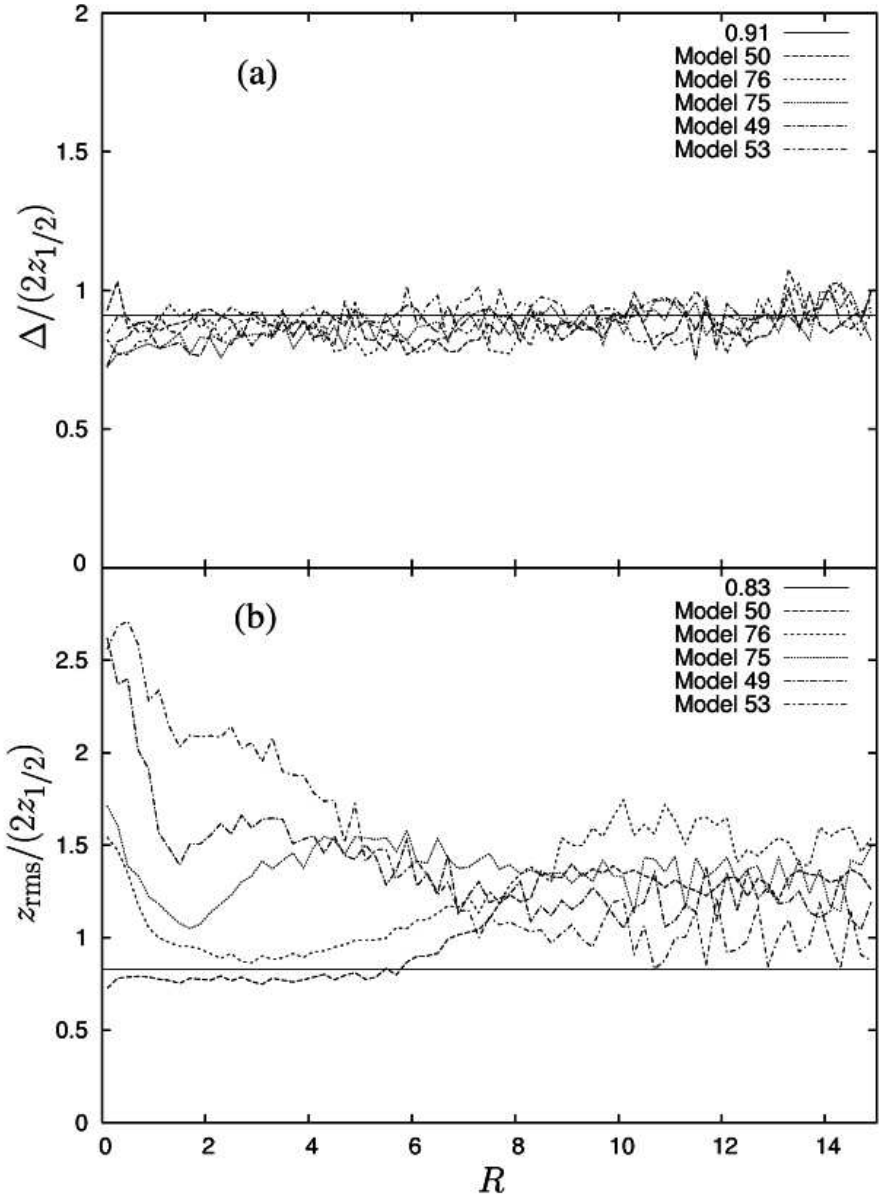

Figure 1: (a) $\Delta/(2z_{1/2})$ vs. R for several models. The solid line indicates the theoretical value of 0.91 for this ratio for density profile (1). All models have the same mass of the spherical component and differ only in mass distribution of this component between the bulge and the halo (the models are listed in order of increasing bulge mass fraction). For all models, $M_{\rm sph}(4h)/M_{\rm d}(4h) = 0.5$ and $h = 3.5$ kpc. (b) $z_{\rm rms}/(2z_{1/2})$ vs. R for the same models. The solid line indicates the theoretical value of 0.83 for this ratio for density profile (1).

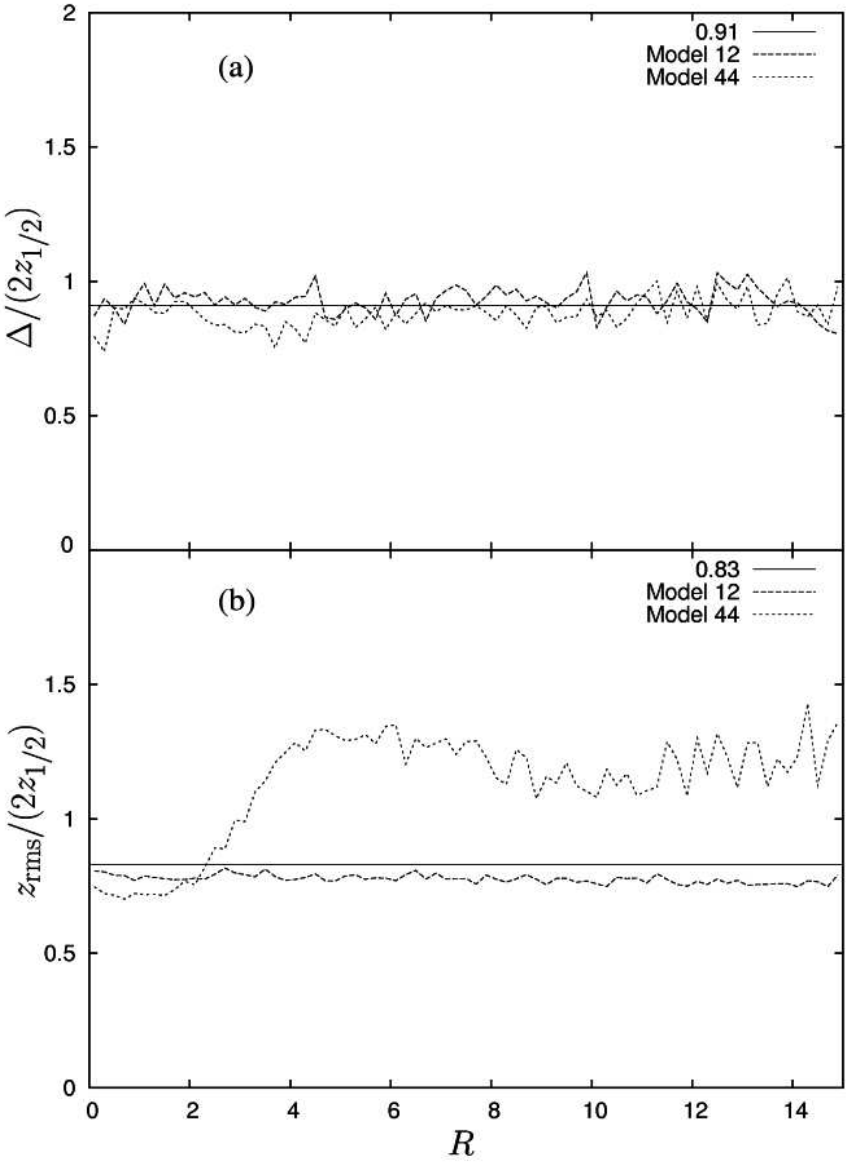

Figure 2: Same as Fig. 1 for two other models – with relatively massive (model 44) and very massive (model 12) spherical components. These models are bulgeless. For models 44 and 12, $\mu(4h) = 1.5$ and $\mu(4h) = 3.43$, respectively; $h = 3.5$ kpc.

vertical density profile can be fitted. Figures 1 and 2 show the azimuthally averaged radial profiles of the ratios $\Delta/2z_{1/2}$ and $z_{\rm rms}/2z_{1/2}$ for several dynamical stellar disk models.

We see from Figs. 1a and 2a that the ratio $\Delta/2z_{1/2}$ is almost constant along the radius for various models. Note that the particle parameters from different parts of the disk are used to determine $z_{1/2}$, Δ, and $z_{\rm rms}$. When $z_{1/2}$ is estimated, it does not matter how extended the tail of distant particles is, but the number of particles that contribute to $z_{1/2}$ is large and accounts for exactly one half of all particles. The volume density produced by only those particles that are located near the main plane of the galaxy and the total surface density are used to calculate Δ; the positions of all the remaining particles do not affect in any way the determination of Δ. As regards $z_{\rm rms}$, all particles, including those that randomly flew far away from the disk plane, contribute to this quantity. It follows from the constancy of the ratio $\Delta/2z_{1/2}$ that these two quantities are adequate estimates of the model disk thickness; otherwise, it would be difficult to explain the coherent behavior of these quantities. At the same time, the equality of this ratio to 0.9 is an argument for the fact that the vertical density profile of stellar disks is similar to law (1) or (6).

As follows from Figs. 1b and 2b, $z_{\rm rms}/2z_{1/2}$ varies significantly along the radius R for all of the analyzed models and, in addition, this ratio is almost always systematically higher than that given by theoretical relations (12), (13), and even (14). The thickness overestimation strongly depends on the degree of matter concentration in the spherical component and on its relative mass. It is different in different parts of the disk. The differences are largest for the models with bulges. For them, the disk thickness in a region of the order of two exponential disk scale lengths can be overestimated by 100% or more (models 49 and 53, Fig. 1b) if $z_{\rm rms}$ is used. As regards regions of more than two radial disk scale lengths, the thickness is overestimated here by 50% or more. For the models with a relative mass of the spherical component $\mu(4h) \leq 1.5$ without a bulge (models 50 and 44, Figs. 1b and 2b), the thickness of the central regions is more or less adequately described by the parameter $z_{\rm rms}$. In this case, the density profile corresponds to isothermal law (1), for which $z_{\rm rms}/2z_{1/2} \approx 0.8$. However, at distances larger than one or one and a half radial exponential disk scale lengths, the thickness proves to be grossly overestimated, approximately by 50%. Only for the models with $\mu(4h) \gtrsim 3.0$ (model 12, Fig. 2b) does $z_{\rm rms}$ serve as a good estimate of the thickness. In addition, the $z_{\rm rms}$ fluctuations along R for the model disks are too large even when a large number of particles is used, in contrast to $z_{1/2}$ (Sotnikova and Rodionov 2005). The ratio $z_{\rm rms}/2z_{1/2}$ also exhibits the same large fluctuations.

The parameter z_0 is commonly used to analyze observational data by assuming the vertical density profile to be isothermal. For our numerical models, we can determine z_0 via both $z_{\rm rms}$ ($z_0 \approx 1.10\, z_{\rm rms}$) and $z_{1/2}$ ($z_0 \approx 1.82\, z_{1/2}$). As we see from the plots of the radial disk thickness profile (Figs. 3a and 3c), z_0 calculated via $z_{\rm rms}$ is considerably larger than z_0 calculated via $z_{1/2}$. Figures 3b and 3d show the vertical density profiles at a given radius ($R = 3.5$ kpc, which corresponds to the exponential radial disk scale length) and the fit to the density profile by isothermal law (1) with the parameter z_0 calculated as $z_0 \approx 1.10\, z_{\rm rms}$ and as $z_0 \approx 1.82\, z_{1/2}$. We see that if z_0 is determined via $z_{1/2}$, then law (1) fits excellently the vertical density profile in the model. When z_0 is determined via $z_{\rm rms}$, the discrepancies between the profiles are enormous.

The above arguments lead us to the following conclusion: the parameter $z_{1/2}$ should be

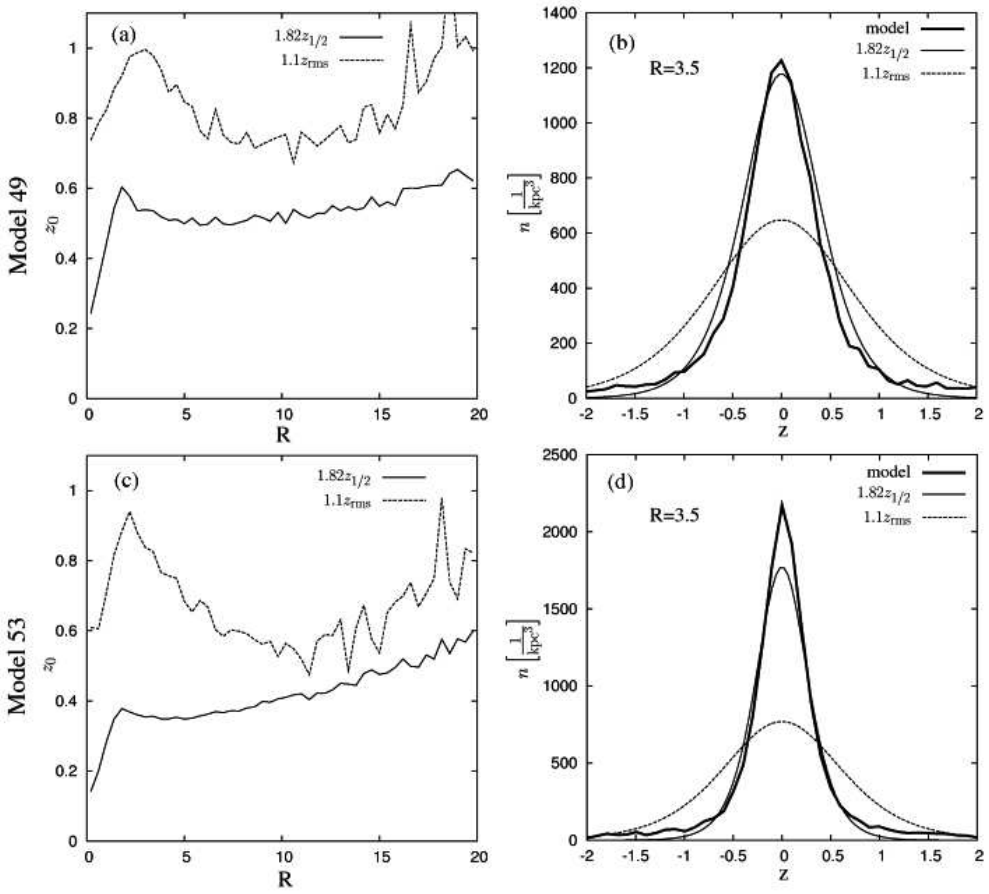

Figure 3: Comparison of the disk thicknesses calculated using $z_{\rm rms}$ and $z_{1/2}$ for two models at the time $t = 5000$ Myr. Models 49 and 53 have $M_{\rm sph}(4h)/M_{\rm d}(4h) = 0.5$, where $h = 3.5$ kpc, but differ in bulge mass fraction (it is larger for model 53). (a), (c) z_0 vs. R; the solid and dashed lines represent z_0 estimated as $1.82\,z_{1/2}$ and $1.10\,z_{\rm rms}$, respectively. (b), (d) Vertical particle density profiles at the radius $R = 3.5$ kpc; the thick solid line represents the profile obtained from the model; the thin solid line represents profile (1) in which z_0 was estimated via $z_{1/2}$; the dashed line represents profile (1) in which z_0 was estimated via $z_{\rm rms}$. The disk surface density at a given distance R in Eq. (1) was calculated from the model.

taken as the stellar disk thickness to analyze the relationships between the disk thickness and other global parameters of galaxies in numerical models. Using $z_{\rm rms}$ can distort significantly the relationship between the relative thickness of a marginally stable stellar disk and the relative mass of the spherical component and can raise the lower limit for the dark halo mass. Below, we use $1.82\,z_{1/2}$, since it corresponds to z_0 for density profile (1).

3.3 Analysis of numerical simulation results

In deriving Eq. (5) for the ratio of the vertical and radial velocity dispersions, we used the value given by the local linear criterion (Toomre 1966; Kulsrud et al. 1971; Polyachenko and Shukhman 1977; Araki 1985). However, the saturation level of the bending instability in numerical simulations can be considerably higher than this value (see, e.g., Sellwood and Merritt 1994; Merritt and Sellwood 1994; Sotnikova and Rodionov 2003). This probably explains why the relationship in Zasov et al.(1991) and Mikhailova et al.(2001) lies above the "theoretical" one.

The ratio σ_z/σ_R at which the bending instability is saturated depends primarily on whether the system admits the growth of global modes. If the growth of global modes is suppressed, then the ratio σ_z/σ_R at a given radius is determined by the local conditions and is equal to its value that follows from the linear criterion. If, however, global modes are possible in the system, then the level of vertical disk heating can be considerably higher.

Sweeping throughout the disk, the global modes cause the ratio σ_z/σ_R to increase to 0.6 and, in central disk regions, to $0.7-0.9$ (Sotnikova and Rodionov 2003). In Fig. 4, the ratio σ_z/σ_R is plotted against the maximum amplitude of bending modes in the time interval from 0 to 3000 Myr for the distance $R = 2h$. The plot was constructed using numerical simulations of disk galaxies. We see a clear correlation between the maximum amplitude of the growing and propagating (through the disk) perturbation and the instability saturation level and, accordingly, the final $\sigma_z(2h)/\sigma_R(2h)$. When global modes are possible in the system, the maximum perturbation amplitude turns out to be larger.

For inhomogeneous disks, the possibility of the growth and propagation of global modes is determined by the conditions in the central disk regions (Sellwood 1996; Sotnikova and Rodionov 2005). These conditions impose constraints on the vertical oscillation frequencies related to the spherical component and the disk and for the model with $\mu(4h)\lesssim 2.0$ depend not only on μ, but also on the degree of matter concentration in the spherical component toward the center (Sotnikova and Rodionov 2005). A low-mass compact bulge suppresses the growth of global bending modes as effectively as a massive dark halo with a large scale length of the matter distribution.

In Fig. 5a, $\sigma_z(2h)/\sigma_R(2h)$ is plotted against the relative mass of the spherical component $\mu(4h)$ for a stellar disk that came to equilibrium after the saturation of the bending instability ($t = 5000$ Myr). It should be noted that a difficulty with the determination of the exponential stellar disk scale length h arises when constructing this plot. During the evolution, an appreciable mass redistribution takes place in many models. The density in the central region can increase greatly. The most significant changes are observed in the models with the formation of a bar. As a result, the density profile in these central

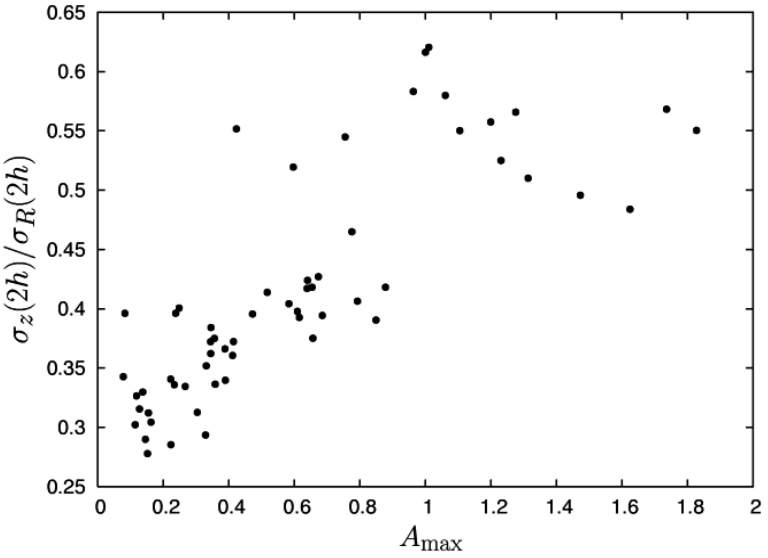

Figure 4: $\sigma_z(2h)/\sigma_R(2h)$ determined at the time $t = 3000$ Myr vs. maximum disk warp amplitude $A_{\max}$ for the period from 0 to 3000 Myr (the disk region within 10 kpc was considered).

regions was fitted by an exponential law with a considerably smaller scale length than that of the density profile on the periphery. For our analysis, we took the exponential scale length estimated from the periphery of a model disk (the region from 5 to 10 kpc), Fig. 5a. For comparison, Fig. 5b shows the same plot, but the value of h was taken at the initial time ($h = 3.5$ kpc for all models at the initial time). The total mass within $4h$ also varies with h. This explains the differences in the ranges of $\mu(4h)$ for the same set of models in Figs. 5a and 5b. The squares in both figures indicate the data for the models with a bulge whose mass is several times lower than the disk mass. Irrespective of $\mu(4h)$, the minimum value of $\sigma_z(2h)/\sigma_R(2h)$ obtained from the models satisfies the linear criterion for bending instability, $(0.29 - 0.37)$. This minimum value corresponds to the models with a compact bulge or a massive halo.

The stabilizing role of a compact bulge lies in the fact that it inhibits the growth of large-scale high amplitude perturbations. In the models with a low mass spherical component and without a compact bulge, the processes that may be arbitrarily called a "violent" stage of the bending instability proceed during the evolution (for the appearance of a bell mode in hot models with large $Q_{\rm T}$ and the rapid growth of bending instability of the bar in cold disks, see Sotnikova and Rodionov (2003)). The physics of these processes may not be directly related to the physics of the bending instability. A vertical resonance can appear in such models (Combes and Sanders 1981; Combes et al.1990; Pfenniger and Friedli 1991; Patsis et al.2002). Nevertheless, these processes affect σ_z/σ_R — it becomes considerably higher than that given by the linear criterion for bending instability.

In Fig. 6a, $z_0(2h)/h$ is plotted against $\mu(4h)$ at the time $t = 5000$ Myr for h calculated from the region from 5 to 10 kpc. Figure 6b shows the same plot for an initial value of $h = 3.5$ kpc. As expected, at fixed relative mass of the spherical component $\mu(4h)$, the models with bulges can be considerably thinner than the models without bulges

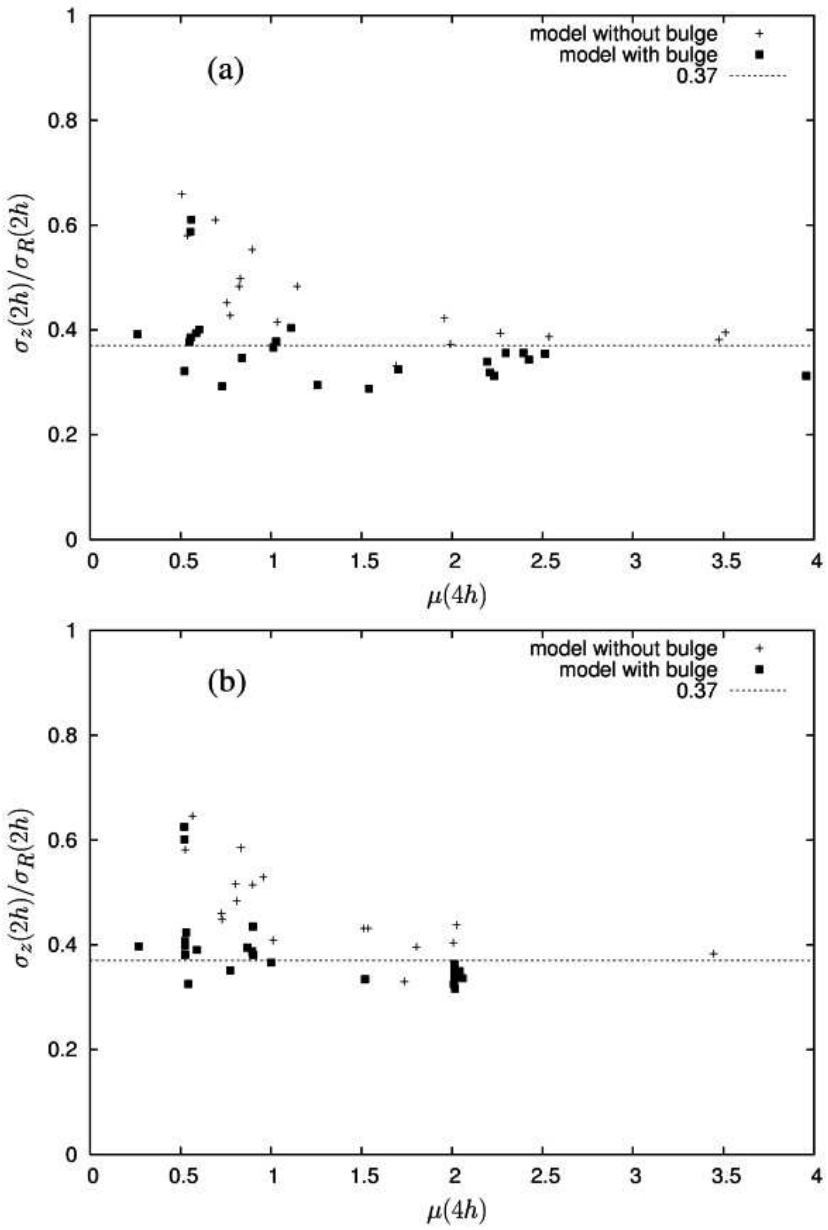

Figure 5: $\sigma_z(2h)/\sigma_R(2h)$ vs. $\mu(4h)$ for our models at the time $t = 5000$ Myr. The crosses and squares indicate the models without and with a bulge, respectively. The dashed line indicates $\sigma_z/\sigma_R = 0.37$ that corresponds to the saturation level of the bending instability derived from the linear criterion of Polyachenko and Shukhman (1977). (a) The exponential disk scale length h was calculated from the model by the least-squares method; the disk region of $R \geq 5$ kpc and $R \leq 10$ kpc was used to calculate h. (b) The initial exponential disk scale length $h = 3.5$ kpc was taken as h.

(see Figs. 6a and 6b). This effect is most pronounced for the models with a spherical component of low relative mass ($\mu(4h) \lesssim 1$).

The following result proved to be more unexpected. The analytical relation between the minimum possible $z_0(2h)/h$ for a stable disk and $\mu(4h)$ (see (5)) is a lower envelope for the model data (see Figs. 6a and 6b). In other words, at fixed $\mu(4h)$, $z_0(2h)/h$ for the thinnest model is approximately equal to the value obtained from Eq.(5).

The data points lying on the lower envelope correspond to the models with compact bulges or with massive halos. For such models, the bend was formed in "quiet" regime or was suppressed altogether. In this case, the final value of σ_z/σ_R was also close to the saturation level of the bending instability derived from the linear criterion. If, however, the bending instability in the model grew in "violent" regime, then the final value of σ_z/σ_R could be considerably higher than that given by the linear criterion and, hence, the final thickness of the model galaxy could be much larger than that following from the linear criterion.

Thus, if a compact spherical component that can be represented by both a bulge and a dark halo with a sharp central density peak (a cuspy halo) is present in a real spiral galaxy in its central region, then the bending instability in such a galaxy will grow in quiet regime. In this case, if the galaxy is marginally stable against bending perturbations and perturbations in the pane, then its parameters will obey Eq. (5).

Consequently, we can use only relation (9) to estimate the lower limit for the dark halo mass from the relative thickness of galaxies. We emphasize once again that this relation gives a weak constraint on the dark halo mass, and only on the condition that the galaxy is in equilibrium, even for thin galaxies.

4 Discussion and conclusions

It is well known that for a stellar disk to be stable against perturbations in the plane, the value of σ_R must be higher than a certain critical value (Toomre 1964). On the other hand, the stability against the growth of bending perturbations requires that the ratio σ_z/σ_R be also larger than a certain critical value. Consequently, the value of σ_z is limited below for a stable stellar disk. The presence of a spherical component, for example, a dark halo, has a stabilizing effect and reduces the minimum radial velocity dispersion required for the stability against the growth of perturbations in the plane. It thus follows that the disks embedded in a massive dark halo can have lower values of σ_z and, as a result, can be thinner. These considerations underlie the conclusion about the existence of a relationship between the relative thickness of marginally stable stellar disks, z_0/h, and the relative mass of the spherical component, μ, within a fixed radius (Zasov et al.1991, 2002).

In this paper, we estimated the coefficient in this relationship and wrote the corresponding theoretical relation (5). The relationship was confirmed by N-body simulations of disk galaxies. This theoretical relation can be used to estimate the lower limit for the dark halo mass from the observed thickness of real spiral galaxies (9). However, even for the thinnest galaxies, this relation yields a weak constraint on the dark halo mass (the dark halo mass within four exponential disk scale lengths must be higher than approx-

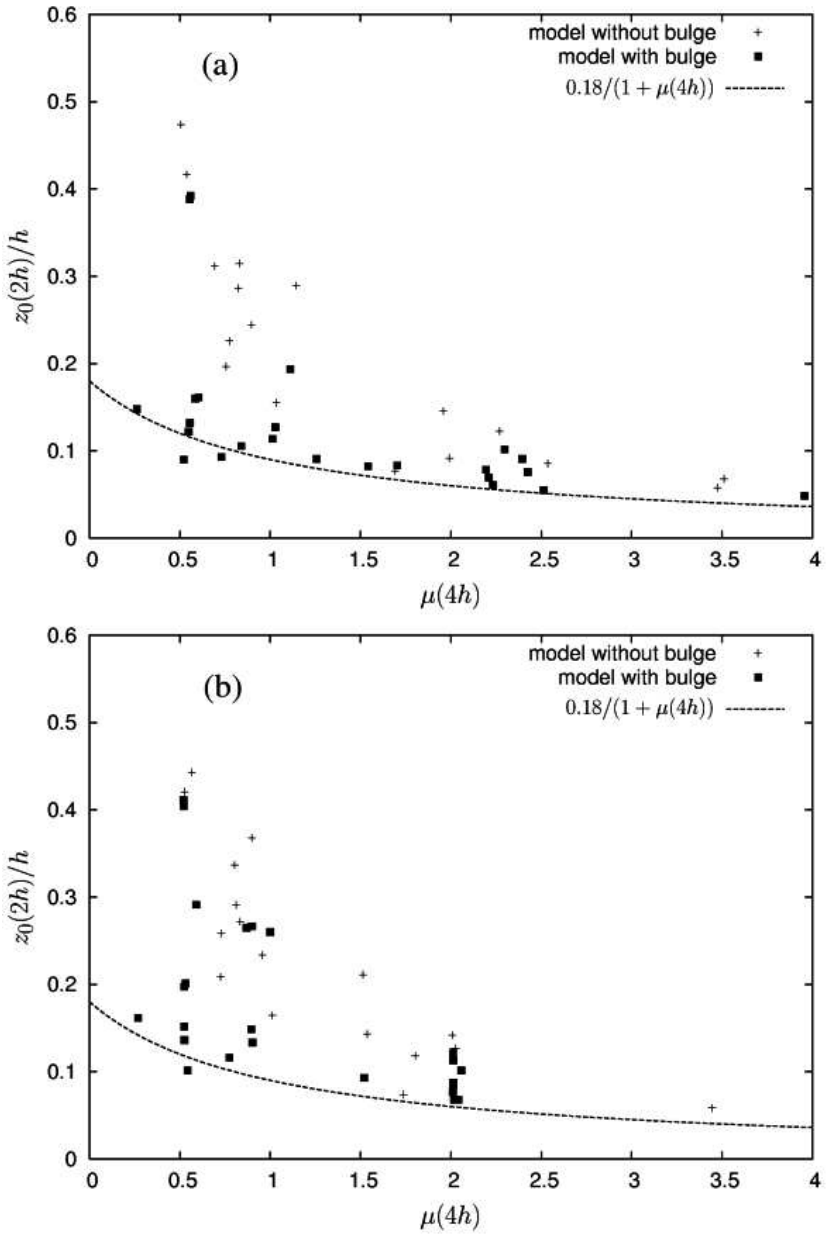

Figure 6: Relative stellar disk thickness at radius $2h$ vs. relative mass of the spherical component within $4h$ for our models at the time $t = 5000$ Myr. The value of z_0 was calculated as $1.82\, z_{1/2}$. The crosses and squares indicate the models without and with a bulge, respectively. The dashed line represents theoretical relation (5). (a) The exponential disk scale length h was determined from the model by the least-squares method; the disk region of $R \geq 5$ kpc and $R \leq 10$ kpc was used to calculate h. (b) The initial exponential disk scale length $h = 3.5$ kpc was taken as h.

imately one disk mass). We can adduce several arguments that will relax this already weak constraint even further.

First, we formally obtain an estimate of the lower limit on the total mass of the galactic spherical component from Eq. (9). The dark halo gives only a partial contribution to this mass. Thus, the dark halo mass estimate becomes even weaker. Second, as was already noted above, in deriving Eq. (5), we assumed that $\sigma_z/\sigma_R = 0.37$, which corresponds to the local linear criterion for bending instability obtained by Polyachenko and Shukhman (1977). However, slightly differing values of this ratio, within the range 0.29 to 0.37, were obtained in different papers in which the bending instability criterion was derived from a local linear analysis. We used the maximum theoretical value for the dispersion ratio. If a smaller ratio is taken, then the coefficient in Eq. (5) will decrease and, as a result, the theoretical estimate of the dark halo mass will also decrease.

Zasov et al. (1991) and Mikhailova et al. (2001) also derived the relationship being discussed from N-body simulations of disk galaxies (in general, the relationships given in these papers coincide). As was already noted above, the model data points in these papers (in contrast to the results of our simulations) lie well above relation (5) and, as a result, the model relation at fixed stellar disk thickness predicts a considerably higher mass of the spherical component than the theoretical relation. What causes these differences? We see three causes.

The main cause of the differences is that the saturation level of the bending instability in simulations can be much higher than the level given by the linear criterion. This is probably the reason why the relationship being discussed derived in the above papers lies above that found from the linear stability criterion for bending perturbations. The numerical simulations by Zasov et al. (1991) and Mikhailova et al. (2001) disregarded the fact that a compact, but not necessarily massive, spherical component could effectively suppress the bending instability. As a result, at fixed total mass of the spherical component, the galaxies with a more concentrated spherical component toward the center (e.g., if there is a compact bulge or a cuspy dark halo in the galaxy) can be considerably thinner than the galaxies with a looser spherical component.

In addition, the overestimation of the model disk thickness is related to the incorrect technique of determining the vertical scale height used in the mentioned papers. It follows from our analysis that the characteristic disk thickness z_0 in numerical simulations must be estimated via the median of the absolute value of z ($z_{1/2}$), not via the rms deviation of the z coorrdinates of particles from the symmetry plane of the disk ($z_{\rm rms}$). Otherwise, the disk thickness can be overestimated significantly, by 100% or more. Thus, the mass of the spherical component determined from the thickness of a marginally stable stellar disk will also be overestimated. Note also that in the mentioned papers, the thickness averaged over the entire disk, including its central regions, was taken when constructing the experimental relationship. This disk-averaged thickness is definitely larger than that calculated on the disk periphery, for example, at the distance $R = 2h$ (for the radial profiles of the final model disk thickness, see Mikhailova et al. (2001) and Sotnikova and Rodionov (2003, 2005)).

The ambiguity of the relationship between the thickness of a galaxy and the mass of its spherical component with different density profiles in numerical simulations complicates the estimation of the dark halo mass from the relative stellar disk thickness z_0/h. However,

to estimate the lower limit for the dark halo mass from the relative thickness of real galaxies, we can use theoretical relation (9), which coincides with the lower envelope of the numerical relationship (Figs. 6a and 6b). This relation gives a weak constraint on the dark halo mass, $\mu(4h) \gtrsim 1$, even for thin galaxies, which is consistent with the upper limits that follow from considerations concerning the conditions for the existence of spiral density waves in galaxies (Athanassoula et al. 1987) and from arguments regarding the extent of tidal features in interacting galaxies (Dubinski et al. 1999).

Acknowledgment
This work was supported by the Russian Foundation for Basic Research (project no. 06-02-16459-a) and a grant from the President of Russia for Support of Leading Scientific Schools (NSh-8542.2006.2).

References

S. Araki, Ph.D., Massachus. Inst. Tech., 1985.

E. Athanassoula, A. Bosma, and S. Papaioannou, Astron. Astrophys **179**, 23(1987).

J. Barnes and P. Hut, Nature **324**, 446(1986).

R. Bottema and J.P.E. Gerritsen, MNRAS **290**, 585(1997).

J.N. Bahcall, Astrophys. J. **276**, 156(1984).

F. Combes, R.H. Sanders, Astron. Astrophys. **96**, 164(1981).

F. Combes, F. Debbasch, D. Friedli, and D. Pfenniger, Astron. Astrophys. **233**, 82(1990).

J. Dubinski, J.Ch. Mihos, and L. Hernquist, Astrophys. J. **526**, 607(1999).

L. Hernquist, Astrophys. J. Suppl. Ser. **86**, 389(1993).

A.V. Khoperskov, A.V. Zasov, and N.V. Tyurina, Astron. Zh. **78** 213(2001) [Astron. Rep. **45** 180(2001)].

A.V. Khoperskov, A.V. Zasov, and N.V. Tyurina, Astron. Zh. **80** 387(2003) [Astron. Rep. **47** 357(2003)].

A.V. Khoperskov and N.V. Tyurina, Astron. Zh. **80** 483(2003) [Astron. Rep. **47** 443(2003)].

M. Kregel, P.C. van der Kruit, and R. de Grijs, MNRAS **334**, 646(2002).

R.M. Kulsrud, J.W-K. Mark, and A. Caruso, Astrophys. Sp. Sci. **14**, 52(1971).

S.S. McGaugh and W.J.G. de Block, Astrophys. J. **499**, 41(1998).

D. Merritt and J.A. Sellwood, Astrophys. J. **425**, 551(1994).

E.A. Mikhailova, A.V. Khoperskov, and S.S. Sharpak, Stellar Dynamics: from Classic to Modern (Eds. L.P. Osipkov and I.I. Nikiforov), St. Petrsburg: St. Petersburg State Univ. Press, 2001, p. 147.

J. Navarro, C.S. Frenk, and S.D.M. White, Astrophys. J. **462**, 563(1996).

P.A. Patsis, E. Athanassoula, P. Grosbol, and Ch. Skokos, MNRAS **335**, 1049(2002).

D. Pfenniger and D. Friedli, Astron. Astrophys. **252**, 75(1991).

V.L. Poliachenko and I.G. Shukhman, Pis'ma Astron. Zh. **3**, 254(1977) [Sov. Astron. Lett. **3**, 134(1977)].

S.A. Rodionov and N.Ya. Sotnikova, Astron. Zh. **82**, 527(2005) [Astron. Rep. **49**, 470(2005)].

S.A. Rodionov and N.Ya. Sotnikova, Astron. Zh., 2006 (in press).

J.A. Sellwood, Astrophys. J. **473**, 733(1996).

J.A. Sellwood and D. Merritt, Astrophys. J. **425**, 530(1994).

N.Ya. Sotnikova, V.P. Reshetnikov, Pis'ma Astron. Zh. **24** 97(1998) [Astron. Lett. **24** 73(1998)]

N. Ya. Sotnikova and S. A. Rodionov, Pis'ma Astron. Zh. **29**, 367(2003) [Astron. Lett. **29**, 321(2003)]

N. Ya. Sotnikova and S. A. Rodionov, Pis'ma Astron. Zh. **31**, 17(2005) [Astron. Lett. **31** 15(2005)]

L. Spitzer, Astrophys. J. **95**, 325(1942).

P.J. Teuben, ASP Conf. Ser. **77**, 398(1995).

A. Toomre, Astrophys. J. **139**, 1217(1964).

A. Toomre, Geophys. Fluid Dyn. **46**, 111(1966).

T.S. van Albada, J.N. Bahcall, K. Begeman, and R. Sancisi, Astrophys. J. **295**, 305(1985).

P.C. van der Kruit, Astron. Astrophys. **192**, 117(1988).

A.V. Zasov, D.I. Makarov, and E.A. Mikhailova, Pis'ma Astron. Zh. **17**, 884(1991) [Sov. Astron. Lett. **17**, 374(1991)].

A.V. Zasov, A.V. Khoperskov, and N.V. Tyurina, Stellar Dynamics: from Classic to Modern (Eds. L.P. Osipkov and I.I. Nikiforov), St. Petrsburg: St. Petersburg State Univ. Press, 2001, p. 95.

A.V. Zasov, D.V. Bizyaev, D.I. Makarov, and N.V. Tyrina Pis'ma Astron. Zh. **28**, 599(2002) [Astron. Lett. **28**, 527(2002)].

Translated by V. Astakhov